

Semileptonic Hyperon Decays at LHCb

A Brea Rodríguez

Instituto Galego de Física de Altas Enerxías (IGFAE), USC, Rúa de Xoaquín Díaz de Rábago, 15705 Santiago de Compostela, A Coruña (SPAIN)

E-mail: alexandre.brea.rodriguez@cern.ch

Abstract. Semileptonic Hyperon Decays (SHD) allow to test Beyond the Standard Model physics with operators not accessible to kaon decays. In this document we will discuss the prospects of the LHCb experiment to improve the existing measurement of muonic SHD. A background rejection study has been made using the LHCb simulation in order to investigate the power to distinguish between the $\Lambda^0 \rightarrow p\mu^-\bar{\nu}$ decay and its main background, the $\Lambda^0 \rightarrow p\pi^-$ decay. Two variables were explored, and their rejection power was estimated by applying a selection criteria. In addition, the estimated $\Lambda^0 \rightarrow p\mu^-\bar{\nu}$ yield at LHCb was calculated.

1. Introduction

Hyperon are baryons containing one or more strange quarks but no charm, bottom nor top quarks. The aim of this study is to explore the LHCb potential to study Semileptonic Hyperon Decays (SHD) and also discuss their relevance from a theoretical point of view, as well as the need to resume the work on this field, since some of the measurements have not been updated for a long time.

In these proceedings we discuss the current status, which channels are the most interesting ones, given the features of the LHCb detector, and we also present prospects and expected yields.

1.1. LCHb features

The LHCb detector is a single-arm forward spectrometer, covering the pseudo-rapidity range $2 < \eta < 5$, that operates in proton-proton (pp) collisions collecting data at the Large Hadron Collider (LHC) at CERN.

Hyperons are copiously produced at the LHC, which allows to study their properties even without specific trigger selections. Despite having neutrinos in their final state, SHD can be effectively reconstructed using kinematic constrains.

Several types of tracks can be reconstructed at LHCb [1], the most relevant ones being:

- Long tracks: have all the tracking information from the VELO up to the T-stations, implying that the mother particle decayed within ~ 1 m of the pp interaction point;
- Downstream tracks: where only the TT and T-stations registered hits, allowing strange hadrons to be reconstructed with decay lengths up to about 2 m from the pp interaction point.

The use of downstream tracks implies a worse momentum and secondary vertex resolution, but allows to study long-lived particles, specially if some of their daughters are long-lived particles too and can be reconstructed as tracks.



1.2. Relevance and status.

From the theoretical point of view, SHD are very relevant as being sensitive to Beyond the Standard Model (BSM) dynamics that break lepton universality [2]. These decays are controlled by a small SU(3) flavour breaking parameter that allows for systematic expansions and accurate predictions in terms of a reduced dependence on hadronic form-factors. More specifically, muonic modes are very sensitive to non-standard and tensor contributions and these could provide a powerful synergy with direct searches of BSM new physics at the LHC.

On the experimental side, measurements in this field have not been updated in the last decades. For example, the $\Lambda^0 \rightarrow p\mu^-\bar{\nu}$ branching fraction measurement dates back to the 70's. In addition, branching fractions of SHD are affected by uncertainties at the 20 – 100 % level, leaving vast room for progress. For example, $\mathfrak{B}(\Xi^- \rightarrow \Lambda^0\mu^-\bar{\nu}) = 3.5_{-2.2}^{+3.5} \times 10^{-4}$ and $\mathfrak{B}(\Xi^- \rightarrow \Sigma^0\mu^-\bar{\nu}) < 8.0 \times 10^{-4}$ at 90 % CL [3]. Improved measurements directly translate into tighter bounds on Lepton Flavour Universality (LFU), since the electron modes have already been measured very precisely.

Therefore, more experimental and theoretical work, both on SHD and on semileptonic kaon decays, is needed [4].

2. Prospects for measurements with strange hadrons.

Some prospects for measurements with strange hadrons have been recently published [5]. The study was performed using Pythia 8 [6] to generate the decays and employed a fast simulation of the LHCb upgrade tracking system. The results, obtained from a simplified description of the LHCb Upgrade tracking system geometry, are presented in table 1. Channels containing a photon, neutrino and π^0 are partially reconstructed. The acceptance scale factors for charged hadrons with at least 300 MeV/c and electrons with over 200 MeV/c transverse momenta are indicated in parentheses.

Table 1: Acceptance scale factors ϵ , normalised to that of fully reconstructed $K_S^0 \rightarrow \mu^+\mu^-$ (long tracks case), and mass resolutions σ , for only long (L) and only downstream (D) tracks. The production ratio of the strange hadron with respect to K_S^0 is shown as \mathcal{R} .

Channel	\mathcal{R}	ϵ_L	ϵ_D	σ_L (MeV/c ²)	σ_D (MeV/c ²)
$K_S^0 \rightarrow \mu^+\mu^-$	1	1.0 (1.0)	1.8 (1.8)	~ 3.0	~ 8.0
$K_S^0 \rightarrow \pi^+\pi^-$	1	1.1 (0.30)	1.9 (0.91)	~ 2.5	~ 7.0
$K_S^0 \rightarrow \pi^0\mu^+\mu^-$	1	0.93 (0.93)	1.5 (1.5)	~ 35	~ 45
$K_S^0 \rightarrow \gamma\mu^+\mu^-$	1	0.85 (0.85)	1.4 (1.4)	~ 60	~ 60
$K_S^0 \rightarrow \mu^+\mu^-\mu^+\mu^-$	1	0.37 (0.37)	1.1 (1.1)	~ 1.0	~ 6.0
$K_L^0 \rightarrow \mu^+\mu^-$	~ 1	$2.7 (2.7) \times 10^{-3}$	0.014 (0.014)	~ 3.0	~ 7.0
$K^+ \rightarrow \pi^+\pi^+\pi^-$	~ 2	$9.0 (0.75) \times 10^{-3}$	$41 (8.6) \times 10^{-3}$	~ 1.0	~ 4.0
$K^+ \rightarrow \pi^+\mu^+\mu^-$	~ 2	$6.3 (2.3) \times 10^{-3}$	0.030 (0.014)	~ 1.5	~ 4.5
$\Sigma^+ \rightarrow p\mu^+\mu^-$	~ 0.13	0.28 (0.28)	0.64 (0.64)	~ 1.0	~ 3.0
$\Lambda \rightarrow p\pi^-$	~ 0.45	0.41 (0.075)	1.3 (0.39)	~ 1.5	~ 5.0
$\Lambda \rightarrow p\mu^-\bar{\nu}_\mu$	~ 0.45	0.32 (0.31)	0.88 (0.86)	–	–
$\Xi^- \rightarrow \Lambda\mu^-\bar{\nu}_\mu$	~ 0.04	$39 (5.7) \times 10^{-3}$	0.27 (0.09)	–	–
$\Xi^- \rightarrow \Sigma^0\mu^-\bar{\nu}_\mu$	~ 0.03	$24 (4.9) \times 10^{-3}$	0.21 (0.068)	–	–
$\Xi^- \rightarrow p\pi^-\pi^-$	~ 0.03	0.41 (0.05)	0.94 (0.20)	~ 3.0	~ 9.0
$\Xi^0 \rightarrow p\pi^-$	~ 0.03	1.0 (0.48)	2.0 (1.3)	~ 5.0	~ 10
$\Omega^- \rightarrow \Lambda\pi^-$	~ 0.001	$95 (6.7) \times 10^{-3}$	0.32 (0.10)	~ 7.0	~ 20

The $\Lambda^0 \rightarrow p\mu^-\bar{\nu}$ channel has a high production ratio and high acceptances compared to the other hyperon decays, which makes it one of the most interesting channels to study SHD. In this case the expected yield is large, which means that the main challenge is not the trigger efficiency, but the discrimination against peaking backgrounds.

The main background associated to this channel is the $\Lambda^0 \rightarrow p\pi^-$ decay, with a branching fraction of 63.9 %, in which the pion is misidentified as a muon.

The strategy to discriminate against peaking backgrounds is to identify a plane where signal and background show different behaviours. Analogous studies were performed, for the $\Lambda^0 \rightarrow p\mu^-\bar{\nu}$ and $\Xi^- \rightarrow \Lambda^0\mu^-\bar{\nu}$ channels, to demonstrate the expected capacity of the LHCb detector to carry out these analyses.

Figure 1 shows the result of a fast simulation, in which the final state radiation in the decay vertex is not included [5]. Two variables were explored, the reconstructed invariant mass (M) and the missing momentum in the plane transverse to the mother flight direction (p_T).

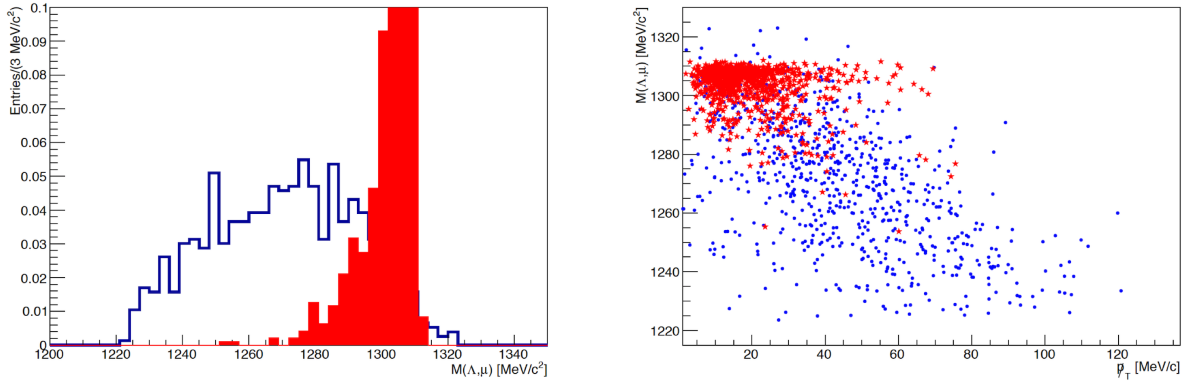


Figure 1: The left plot shows the reconstructed invariant mass for $\Xi^- \rightarrow \Lambda^0\mu^-\bar{\nu}$ candidates (events normalized to unity). Signal events are given by a solid blue line, while the $\Xi^- \rightarrow \Lambda^0\pi^-$ background is displayed in filled red. The right figure shows a scatter plot of M vs. p_T for signal (blue) and $\Xi^- \rightarrow \Lambda^0\pi^-$ background (red).

Signal and background exhibit contrasting signatures, both in the $\Lambda^0 \rightarrow p\mu^-\bar{\nu}$ and in the $\Xi^- \rightarrow \Lambda^0\mu^-\bar{\nu}$ case [5]. These results should be verified by using the LHCb simulation framework.

3. Theoretical model

In order to generate correctly our simulated signal sample we must use the proper theoretical expressions for the differential decay rate.

The differential decay rate for Semileptonic Hyperon Decays can be obtained from [2]:

$$\frac{d\Gamma}{dq^2 d(\cos\theta)} = \frac{G_F^2 f_1(0)^2 |V_{us}|^2}{(2\pi)^3} (q^2 - m_l^2)^2 \frac{q_3 \Delta^2}{16q^2} [I_1(q^2) + I_2(q^2)\cos(\theta) + I_3(q^2)\cos^2(\theta)] \quad (1)$$

where q^2 is the invariant mass squared of the lepton pair, $f_1(0)$ the vector coupling, θ the angle between the neutrino 3-momentum and the recoiling baryon direction of flight (in the dilepton rest-frame), $\Delta = M_1 - M_2$, with $M_1(M_2)$ the parent (daughter) baryon mass, $\delta = \frac{M_1 - M_2}{M_1}$ and the angular coefficients of the 3-body decay being

$$I_1e = \frac{4(1-\delta)}{q^2} \left((1 - \frac{q^2}{\Delta^2}) + (1 + \frac{q^2}{\Delta^2}) (\frac{g_1(0)}{f_1(0)})^2 \right), \quad I_1\mu = \frac{4m_l^2}{q^4} (1-\delta) \left(1 + (\frac{g_1(0)}{f_1(0)})^2 \right) \quad (2)$$

$$I_2e = \frac{8\delta}{\Delta^2} \sqrt{1 - \frac{q^2}{\Delta^2}} \left(1 + 2 \frac{f_2(0)}{f_1(0)} \right) \frac{g_1(0)}{f_1(0)}, \quad I_2\mu = -\frac{8m_l^2}{q^4} \sqrt{1 - \frac{q^2}{\Delta^2}} (1-\delta) \left(1 + (\frac{g_1(0)}{f_1(0)})^2 \right) \quad (3)$$

$$I_3e = -\frac{4(1-\delta)}{q^2}\left(1 - \frac{q^2}{\Delta^2}\right)\left(1 + \frac{g_1(0)}{f_1(0)}\right)^2, \quad I_3\mu = \frac{4m_l^2}{q^4}\left(1 - \frac{q^2}{\Delta^2}\right)(1-\delta)\left(1 + \left(\frac{g_1(0)}{f_1(0)}\right)^2\right) \quad (4)$$

where $g_1(0)$ and $f_2(0)$ are the axial-vector and weak-magnetic couplings, respectively. Hence, $I_i = I_i e + I_i \mu$ ($i=1,2,3$). Finally, q_3 can be calculated by

$$q_3(M_1, M_2) = \frac{1}{2M_1} \sqrt{M_1^4 + M_2^4 + q^4 - 2(M_1^2 M_2^2 + q^2 M_1^2 + q^2 M_2^2)} \quad (5)$$

The inputs are obtained from data or systematically in a SU(3)-breaking expansion. More precisely: $f_1(0)$ is connected by SU(3) to the charges of proton and neutron and is protected from leading corrections by the Ademollo-Gatto theorem. $\frac{g_1(0)}{f_1(0)}$ is measured from the energy spectrum in the electronic modes and $f_2(0)$ is related by SU(3) with the magnetic moments of proton and neutron (corrections enter at Δ^2 in the rate). The numbers are presented in Tab. 2:

Table 2: Coefficient values for the $\Lambda^0 \rightarrow p\mu\nu$ decay.

Channel	$f_1(0)$	$\frac{g_1(0)}{f_1(0)}$	$\frac{f_2(0)}{f_1(0)}$
Λp	$-\sqrt{\frac{3}{2}}$	0.718	1.066

Using these expressions and coefficient values we have everything we need to start generating Monte Carlo (MC) events with the proper theoretical model.

4. Selection Efficiency

Once we generate the MC events, we can obtain the selection efficiency.

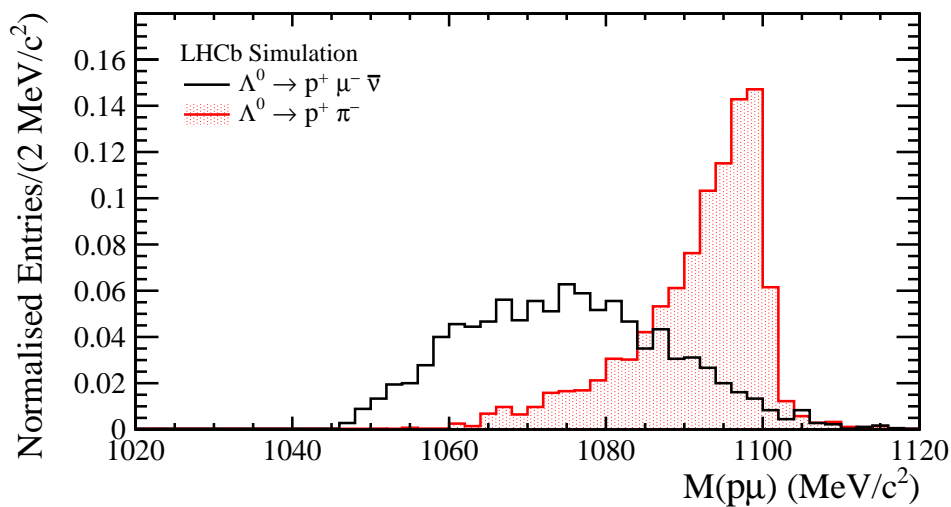


Figure 2: Reconstructed invariant mass under the proton-muon hypothesis ($M(p\mu)$). The $\Lambda^0 \rightarrow p\mu^- \bar{\nu}$ candidates are given by a solid black line, while the $\Lambda^0 \rightarrow p\pi^-$ background is displayed in filled red. The histograms areas are normalised.

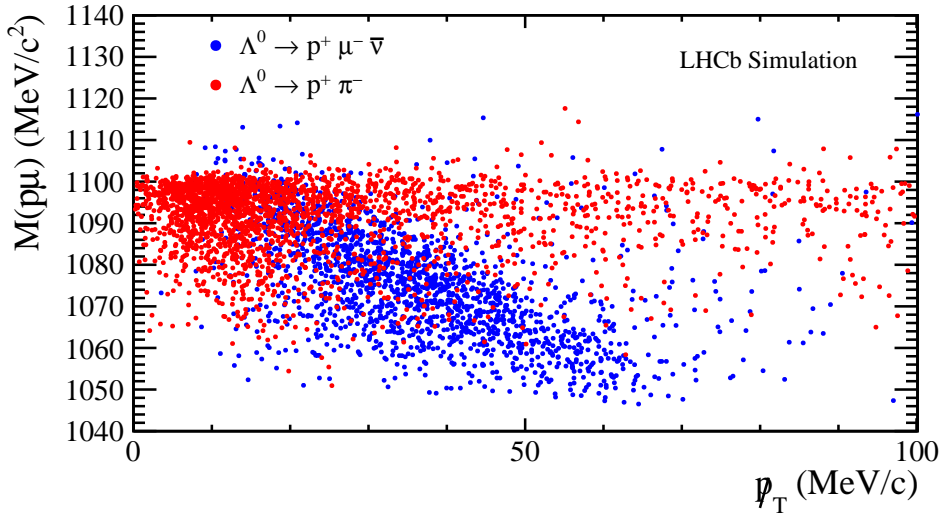


Figure 3: Scatter plot of the Reconstructed Mass vs. the Missing Momentum in the plane transverse to the Λ^0 flight direction for signal (in blue) and background (in red).

The explored variables in Fig. 2 and Fig. 3 were suggested to separate between $\Lambda^0 \rightarrow p\mu^-\bar{\nu}$ and its main background, $\Lambda^0 \rightarrow p\pi^-$ [5]. In fact, from the LHCb simulation [7], we verify that the channels have contrasting signatures. In Table 3 the estimated results of a selection criteria are shown.

Table 3: Selection requirements in the $M(p, \mu)$ vs \not{p}_T plane and its estimated results.

Cut in \not{p}_T	Cut in $M(p\mu)$	$\Lambda^0 \rightarrow p\pi^-$ rejected	Signal selected (ϵ_{Sel})
$\not{p}_T > 25 \text{ MeV}/c$	$M(p\mu) < 1080 \text{ MeV}/c^2$	94.8 %	58.7 %

5. Expected Yield

In Figure 4 [7], we can see the invariant mass spectrum for our normalization channel, $\Lambda^0 \rightarrow p\pi^-$, and its charge-conjugated decay, selected from a LHCb data sample. In this case, the $\Lambda^0 \rightarrow p\pi^-$ is Trigger Independent of Signal (TIS), which implies that for each candidate the rest of the event is sufficient to generate a positive trigger decision.

From Fig. 4 we obtain a measured $\Lambda^0 \rightarrow p\pi^-$ yield of 65.2×10^6 per fb^{-1} at LHCb. Assuming the same trigger efficiency for both, $\Lambda^0 \rightarrow p\pi^-$ and $\Lambda^0 \rightarrow p\mu^-\bar{\nu}$, channels, the expected $\Lambda^0 \rightarrow p\mu^-\bar{\nu}$ yield is given by the following expression:

$$N(\Lambda^0 \rightarrow p\mu^-\bar{\nu}) = N(\Lambda^0 \rightarrow p\pi^-) \times \frac{\mathfrak{B}(\Lambda^0 \rightarrow p\mu^-\bar{\nu})}{\mathfrak{B}(\Lambda^0 \rightarrow p\pi^-)} \times \frac{\epsilon_{L(\Lambda^0 \rightarrow p\mu^-\bar{\nu})}}{\epsilon_{L(\Lambda^0 \rightarrow p\pi^-)}} \times \epsilon_{Sel} \quad (6)$$

where ϵ_L are the acceptance efficiencies, extracted from Tab. 1, and ϵ_{Sel} is the estimated selection efficiency for $\Lambda^0 \rightarrow p\mu^-\bar{\nu}$, extracted from Table 3. The current measured branching fractions are $\mathfrak{B}(\Lambda^0 \rightarrow p\mu^-\bar{\nu}) = (1.57 \pm 0.35) \times 10^{-4}$ and $\mathfrak{B}(\Lambda^0 \rightarrow p\pi^-) = (63.9 \pm 0.5) \times 10^{-2}$ [3]. Putting the numbers in Eq. 6, we expect 7330 reconstructed and selected $\Lambda^0 \rightarrow p\mu^-\bar{\nu}$ candidates per fb^{-1} . This implies 44000 candidates in the whole LHCb Run II ($\mathcal{L} = 6.0 \text{ fb}^{-1}$).

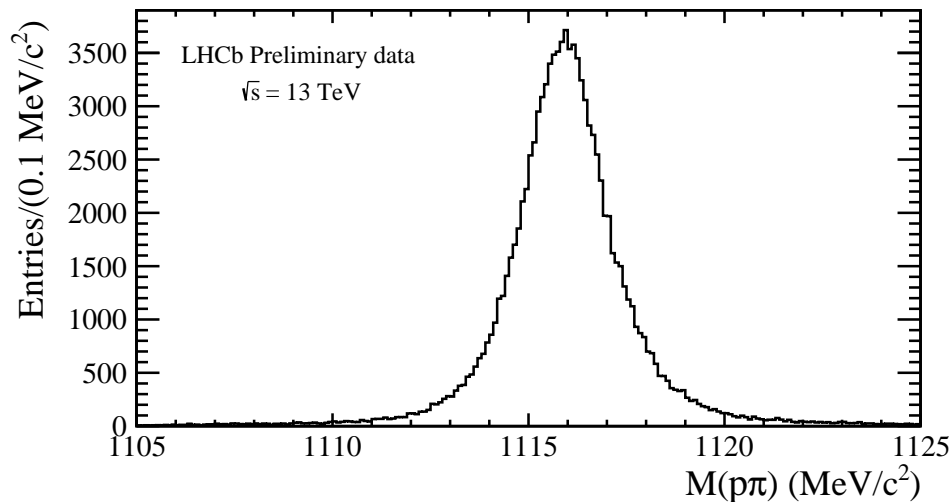


Figure 4: Mass spectrum $M(p\pi)$ at LHCb for $\Lambda^0 \rightarrow p\pi^-$ and its charge-conjugated decay for a data sample corresponding to an integrated luminosity of $\mathcal{L} = 1.6 \text{ fb}^{-1}$, with a trigger prescale (downscaling of the data rate) of 10^{-3} applied. The measured yield is 107320 ± 330 .

6. Conclusions

Semileptonic Hyperon Decays are very interesting from the theoretical point of view, since they can be sensitive to BSM dynamics that break lepton universality and, specifically, their muonic modes are very sensitive to non-standard and tensor contributions [2]. Even having precise theoretical calculations for the branching fractions, measurements on this field have not been updated in the last decades.

Once the ability of the LHCb detector to carry out the SHD analysis was proved, a strategy to separate signal and peaking backgrounds has been proposed in this document, as well as the selection efficiency for the $\Lambda^0 \rightarrow p\mu^-\bar{\nu}$ channel.

The expected yield for this channel is around 7330 reconstructed and selected candidates per fb^{-1} . With this yield, the measurement should be dominated by systematics. The statistical uncertainty should be at the level of 1 % and we should be able to improve the current experimental uncertainty on the branching fraction, which is 23 %.

References

- [1] Aaij R *et al.* 2015 LHCb detector performance *Int. J. Mod. Phys. A* **30** no. 0 1530022
- [2] Chang H M, González-Alonso M and Martin Camalich J 2015 Nonstandard semileptonic hyperon decays *Phys. Rev. Lett.* **114** no. 16 161802
- [3] Tanabashi M *et al.* 2018 Review of particle physics *Phys. Rev. D* **98** no. 3 030001
- [4] Cabibbo N, Swallow E C and Winston R 2003 Semileptonic hyperon decays *Ann. Rev. Nucl. Part. Sci.* **53** 39
- [5] Alves Junior A A *et al.* 2019 Prospects for measurements with strange hadrons at LHCb *J. High Energy Phys.* JHEP05(2019)048
- [6] Sjostrand T, Mrenna S and Skand P Z 2008 A brief introduction to PYTHIA 8.1 *Comput. Phys. Commun.* **178** 852
- [7] LHCb Collaboration 2019 Background rejection study in the search for $\Lambda^0 \rightarrow p^+\mu^-\bar{\nu}$ *LHCb-FIGURE* **2019** 006